ACS Macro Letters

pubs.acs.org/macroletters Letter

Mechanically Promoted Synthesis of Polymer Organogels via Disulfide Bond Cross-Linking

Jorge Ayarza, Zhao Wang, Jun Wang, and Aaron P. Esser-Kahn*

Cite This: *ACS Macro Lett.* 2021, 10, 799–804 Read Online

ACCESS | Metrics & More | Article Recommendations | Supporting Information

ABSTRACT: Mechanically adaptive polymers could significantly improve the life-cycle of current materials. Piezo-polymerization is a novel approach that harnesses vibrational mechanical energy through piezoelectric nanoparticles to generate chemical promoters for linear polymerization and cross-linking reactions. However, the available piezo-polymerization systems rely on reactions forming irreversible covalent bonds. Dynamic covalent linkages could impart further adaptability to these polymeric systems. Here we show the first example of the piezoelectrochemical synthesis of disulfide bonds to form organogels from polymers with thiol side groups. We demonstrate that the reaction proceeds via piezo-oxidation of the thiol to disulfide in the presence of ZnO nanoparticles and iodide anions under mechanical agitation. We use mechanical energy in the form of ultrasound (40 kHz) and low frequency vibrations (2 kHz) to synthesize a variety of organogels from common synthetic polymers. Additionally, we show that the polymers in these gels can be chemically recycled with a reducing agent. Finally, we study the thermal and mechanical properties of the composites obtained after drying the gels. We believe this new system adds to the piezo-polymerization repertoire and serves as the basis to fabricate mechanically adaptive polymeric materials via dynamic covalent bonds.

Synthetic polymeric materials are often subject to continuous mechanical stress, which eventually leads to degradation, bond breakage and failure. Vibrational mechanical energy (>100 J) that is constantly being transmitted through the material is usually detrimental in nature and rarely harnessed for constructive or adaptive purposes.[1−6] Mechanically controlled polymerization reactions are of particular interest for designing smart polymers that strengthen under stresses commonly encountered in many engineering applications.[7−16] Recently, we and others have reported using piezoelectric nanoparticles to directly transduce mechanical energy into chemical energy, which allowed us to conduct polymerization and cross-linking reactions, such as Cu(I)-mediated atom transfer radical polymerization (ATRP), Cu(I) azide−alkyne cycloaddition (CuAAC) step-growth polymerization, Fe-mediated free-radical polymerization, and step-growth thiol−ene polymerization.[17−23]

Building on the work of a growing group of researchers, we and others have reported that piezoelectric nanoparticles, such as $BaTiO_3$ and ZnO, can facilitate electron transfer processes between redox active species, which in turn can be used to generate polymerization or cross-linking promoters. We have previously used this methodology to synthesize organogels from multifunctional monomers or polymers with reactive functionalities.[20,21,23] However, the reactions we have relied on thus far have all led to irreversible covalent bonds between polymer chains. To develop adaptive materials, many systems have employed dynamic linkages that can be selectively formed and broken.[24−26] The thiol−disulfide reaction is a prime example of a reversible reaction that has been extensively used to develop stimuli-responsive and self-healing materials. However, most of the literature has focused on using heat or light for the oxidation of thiols to disulfides or the metathesis of disulfide bonds within a polymer matrix.[27,28] Other reports have shown that mechanical stress (ultrasound or cyclic loading) can cleave polymer-embedded disulfide bonds.[29] Another report showed that under ultrasonication, small-molecule thiols could be oxidized in the presence of air and a stoichiometric amount of a non-nucleophilic base.[30] In this context, we theorized that the thiol−disulfide redox pair (RSH/RSSR) would be a suitable target for nanoparticle-mediated piezoelectrochemistry because of its relatively low standard redox potential. Although $E^{\circ}_{RSH/RSSR}$ is dependent on the substituent on the thiol, reported values for glutathione and cysteine are in the range of −250 to −200 mV.[31] In this work, we demonstrate a mechanically promoted synthesis of organogels via the formation of disulfide linkages between polymers with thiol functionalities. Furthermore, we show that these organogels can be dissolved with a reducing agent, and

Received: May 17, 2021
Accepted: June 6, 2021
Published: June 14, 2021

https://doi.org/10.1021/acsmacrolett.1c00337
ACS Macro Lett. 2021, 10, 799–804

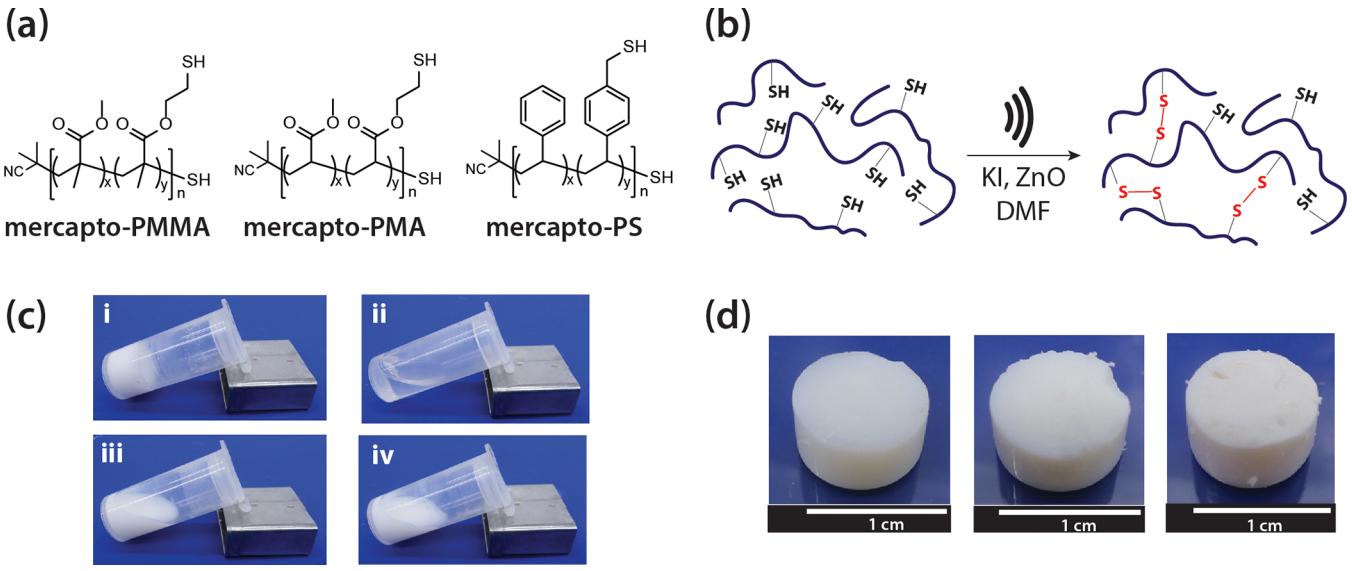

Figure 1. (a) Chemical structures of synthesized polymers with thiol side groups (mercapto-polymers). (b) Reaction scheme for mechanically promoted cross-linking of mercapto-polymers via disulfide bond formation. (c) Pictures of control reactions for the ultrasound-promoted gelation of mercapto-PMMA: (i) all reaction components, (ii) no ZnO, (iii) no ultrasonication (stirring at 100 rpm), and (iv) no KI. Vial dimensions: 0.68 in. × 1.09 in. (d) Pictures of organogels for mercapto-PMMA, mercapto-PMA, and mercapto-PS (from *left* to *right*, respectively).

the recovered polymer can be reused to form another organogel.

To test the formation of disulfide polymeric materials, we started by synthesizing three linear polymers with thiol side groups (Figure 1a): a polymethacrylate variant (mercapto-PMMA), a polyacrylate variant (mercapto-PMA), and a polystyrene variant (mercapto-PS). Mercapto-PMMA and mercapto-PMA were synthesized via reversible addition−fragmentation chain transfer polymerization (RAFT) from a modified literature procedure, and mercapto-PS was synthesized via free-radical polymerization with a thermal initiator.[32] All mercapto-polymers were fully characterized (Supporting Information, Sections 1.2 and 1.3).

Our first goal was to test if these polymers could form organogels via mechanically promoted disulfide bonds formation. We dissolved mercapto-PMMA (150 mg, 1 eq thiol) in dimethylformamide (DMF, 400 μL) and added KI (11 mg, 0.5 eq) and ZnO nanoparticles (Φ = 18 nm, 30 mg, 5 wt %). After homogenizing, the sample was sonicated in an ultrasound bath (40 kHz) for 6 h at room temperature. On the basis of previous literature, we theorized KI would act as an intermediary reagent. In a conventional synthesis of disulfides, KI is oxidized *in situ* with H_2O_2 to form I_2, which subsequently converts thiols to disulfides.[33]

We hypothesized that piezoelectric nanoparticles under mechanical agitation could similarly oxidize iodide anions, thus promoting the oxidation of thiols to disulfides and the cross-linking of the polymers (Figure 1b). The gelation of mercapto-PMMA was confirmed by the inversion test. The gel was allowed to set for 12 h before removing it from the vial. Control experiments were run by selectively removing ZnO and KI (Figure 1c). When we removed either of these substances, no gel was formed. From these results, we made preliminary observations that gelation was mechanically promoted and required not just ZnO but also KI to accelerate the formation of presumably a disulfide bond. Using an analogous procedure, organogels were synthesized from mercapto-PMA and mercapto-PS (Figure 1d). In the case of mercapto-PMA, the amounts of polymer and KI were adjusted to 200 mg and 16 mg, respectively, while in the case of mercapto-PS, they were set at 150 mg and 11 mg, respectively.

After finding increasing evidence that disulfide bonds were the reason behind the cross-linking of the polymers, we studied the reversibility of the gelation. The mercapto-PMMA gel could be dissolved in a solution of tris(2-carboxyethyl)-phosphine hydrochloride (TCEP) in DMF (0.16 M) after mild heating at 50 °C for 12 h (Figure S9). As TCEP is a commonly used reducing agent that converts disulfides into thiols, we hypothesized it would readily solubilize the gels. Nevertheless, there was also the possibility that the ZnO was acting as a binder via coordination with the thiol side groups of the polymer and that the formed disulfides were incidental.[34−36] Therefore, we tested the gel by treating it with a strong acid solution which would dissolve the ZnO but not break the disulfide bonds. As shown in Figure S9, a trifluoroacetic acid (TFA) solution in DMF (0.1 M) does not dissolve the gel, even though the ZnO is solubilized. To serve as a reference, we synthesized a mercapto-PMMA gel via conventional thermal curing. We replaced the ZnO with H_2O_2 (30 vol. %, 2 μL) as the oxidizing agent and heated the sample at 60 °C for 1 h. We tested this gel with both the TCEP and TFA solutions, and only TCEP would dissolve it.

With a working procedure for the mechanically promoted gelation and supporting evidence for the formation of disulfides, we sought to find direct chemical evidence. Since analyzing the gels proved difficult, we used a small molecule thiol in place of the mercapto-polymers and measured the conversion of thiol to disulfide with qNMR. As shown in Figure S10, when benzyl mercaptan (59 μL, 0.5 mmol) was mixed with KI (42 mg, 0.25 mmol) and ZnO (15 mg, 2.5 wt %) in DMF and ultrasonicated, we observed disulfide formation. The GC-MS spectra of the reaction product confirmed the presence of dibenzyl disulfide, and also showed a tiny amount of dibenzyl sulfide (Supporting Information, Section 3). It is possible than some desulfurization might happen at the surface of the ZnO nanoparticles.[34,37] While the

https://doi.org/10.1021/acsmacrolett.1c00337
ACS Macro Lett. 2021, 10, 799−804

conversion of benzyl mercaptan was relatively low at 18%, this much would be sufficient for cross-linking to occur in the mercapto-polymer system. Control reactions in the absence of ZnO, KI or ultrasound resulted in considerably lower yields of disulfide. In addition to the NMR study, the formation of I_2 was confirmed with UV−vis spectroscopy in a similar experiment (Figure S11). These results indicated that all three components were necessary to produce the desired piezoelectrochemical response. We postulate that one plausible mechanism is that the ZnO nanoparticles serve both to activate the thiol via surface interactions and to promote the oxidation of the thiol. As for the KI, one interpretation of the results is a mechanism in which the iodide anions facilitate the oxidation by reacting with the surface of the nanoparticles to form iodine, which can then easily oxidize the thiol to disulfide (Figure S12). However, as the "No KI" control indicated, ZnO by itself can weakly oxidize thiols. Finally, the source of mechanical energy, in this case ultrasound, is necessary for the piezoelectrochemical process to occur.

After concluding that the chemical product was indeed disulfides, we sought to study different gelation conditions (Table 1). Mechanical characterization of the organogels was conducted via dynamic mechanical analysis (DMA) under compression mode (Figures S13−S23). First, using mercapto-PMMA as a representative polymer, the concentration of ZnO was varied between 5.0, 2.5, and 1.0 wt % (Table 1a−c). In all of these cases, gelation occurred after ultrasonication (40 kHz) for 6 h; however, the elastic moduli of the resulting gels decreased along with the concentration of ZnO. In a recently published work, our group showed that an electrodynamic shaker, commonly used for testing the mechanical response of materials to vibrations, could also promote piezoelectrochemical processes (Figure S1).[23] As shown in Table 1d, a mercapto-PMMA gel was also formed by mechanical shaking (2 kHz). Although the frequency of the vibrations was significantly less than in ultrasound, the resulting gel had a comparable elastic modulus to the one synthesized with ultrasound (Table 1a). In addition to these experiments, we also tested the reference gel described before (Table 1e). Its elastic modulus was comparable to the gel obtained using 1 wt % ZnO concentration (Table 1c).

Table 1. Gelation Study of Mercapto-Polymers

sample	polymer	ZnO (wt %)	energy source[a]	E (kPa)[c]
a	mercapto-PMMA	5.0	ultrasound	776
b		2.5	ultrasound	658
c		1.0	ultrasound	178
d		5.0	shaker	760
e[b]		–	heat	42
f	mercapto-PMA	5.0	ultrasound	90
g		5.0	shaker	2
h	mercapto-PS	5.0	ultrasound	570
i		5.0	shaker	202

[a]Conditions: ultrasound bath (40 kHz, 110 W, 6 h), electrodynamic shaker (2 kHz, 130 W, 8 h), and heat (60 °C, 1 h). Gels were allowed to set for 12 h after sonication (or heating). [b]Control reaction: H_2O_2 30 vol. % (2 μL). Shear modulus (G, kPa) measured with rheometer. [c]Young's modulus (E, kPa) determined from the slope of stress−strain curve.

For the mercapto-PMA and mercapto-PS polymer systems, organogels were synthesized using both the ultrasound and the shaker (Table 1, samples **f**−**i**). The mercapto-PMA gel synthesized with ultrasound (40 kHz) had an elastic modulus almost an order of magnitude lower in comparison to the analogous gel with mercapto-PMMA, though it was still solid. However, the gel synthesized via shaking at 2 kHz showed weak consistency after being removed from the vial. Oscillatory strain and frequency measurements confirmed that the sample was cross-linked, but its elastic modulus was comparatively low at 2 kPa (Figure S20). In the case of mercapto-PS, both 40 kHz ultrasound and 2 kHz shaker yielded consistent gels. However, for the shaker case, the elastic modulus was lower by about half. In general, these results indicate that the lower energy output of the shaker in comparison to the ultrasound leads to lower reactivity and thus lower modulus. In summary, we showed that a variety of organogels with different moduli are accessible with this methodology.

To further examine the physical properties of the organogels, we selected representative samples **a**, **f**, and **h**, corresponding to the mechano-cross-linking of mercapto-PMMA, mercapto-

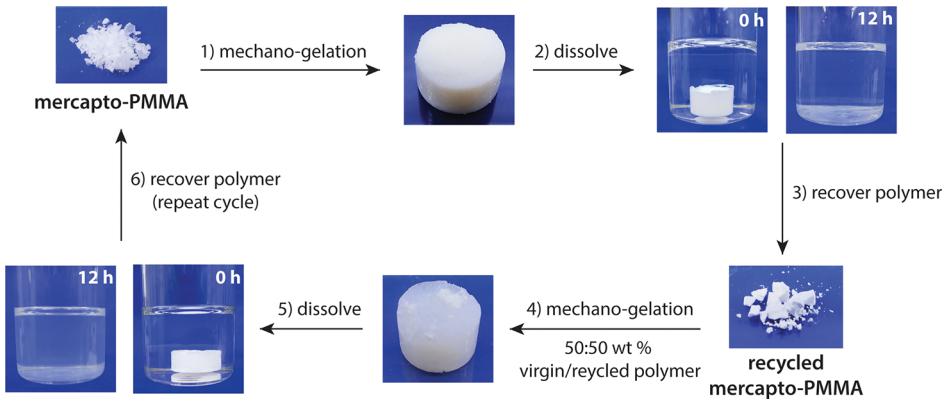

Figure 2. Recyclability study of mercapto-PMMA organogel. (1) Mercapto-PMMA (150 mg) and KI (11 mg) were dissolved in DMF (400 μL) and mixed with ZnO nanoparticles (30 mg, 5 wt %). The mixture was ultrasonicated (40 kHz) for 6 h, and the gel was left to set for 12 h. (2) The gel was placed in a solution of TCEP in DMF (8 mL, 0.16 M) and stirred at 50 °C for 12 h. (3) The solution was centrifuged at 10k rpm to remove the ZnO nanoparticles and concentrated under vacuum, and the polymer was precipitated in methanol (30 mL), washed, and dried at 60 °C for 24 h. (4) Virgin mercapto-PMMA (75 mg), recycled mercapto-PMMA (75 mg), and KI (11 mg) were dissolved in DMF (400 μL) and mixed with ZnO nanoparticles (30 mg, 5 wt %). The mixture was ultrasonicated (40 kHz) for 6 h and the gel was left to set for 12 h. (5 and 6) Same dissolution and recovery procedure as described above.

https://doi.org/10.1021/acsmacrolett.1c00337
ACS Macro Lett. 2021, 10, 799−804

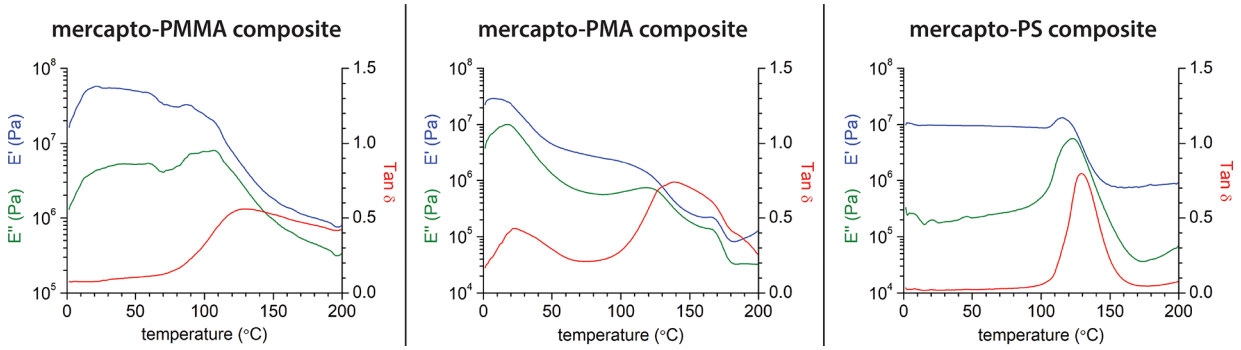

Figure 3. DMA temperature ramp experiments (compression mode) of mercapto-polymer composites in the range of 0−200 °C.

PMA, and mercapto-PS with ZnO (5 wt %) and ultrasound (40 kHz), respectively. The gel fractions were determined by extraction of the soluble polymer with DMF. The mercapto-PMMA gel showed the highest gel fraction at 93%, meanwhile, the mercapto-PMA and mercapto-PS gels showed similar values at 80% and 83%, respectively. Additionally, swelling experiments in DMF showed a nearly a 5× increase in mass of the mercapto-PMA sample due to solvent absorption, in comparison to the 1.8× and 1.5× increments for mercapto-PMMA and mercapto-PS, respectively (Table S4, Figure S24). Finally, we conducted DMA temperature ramp experiments on the gels from −75 to +75 °C (Figures S13, S19, and S21). All samples showed a rubbery plateau around room temperature. The mercapto-PMMA and mercapto-PS gels showed glass transition temperatures (T_g) at −41 and −46 °C, respectively. The mercapto-PMA gel showed no glass transition in the measured temperature range. These results suggest that the mercapto-PMMA gel had a higher degree of cross-linking in comparison to the others. Moreover, the mercapto-PMA gel showed more favorable polymer−solvent interactions in DMF, as it is shown to retain a higher volume of solvent. The comparatively low modulus of the mercapto-PMA gel at room temperature can be attributed to the fact that its T_g appears to be considerably lower than for the other gels.

In previous experiments, we examined the potential gel dissolution to prove the formation of disulfide linkages. However, we were also intrigued that disulfide cleavage could be used as a mechanism for polymer recyclability and processability. To test this idea, we subjected the mechanically cross-linked mercapto-PMMA gel to TCEP reduction. We obtained mercapto-PMMA back from the solution, with a recovery yield of 70 wt % (Figure 2). However, the recycled polymer showed lesser solubility in organic solvents, including DMF, than the virgin polymer. NMR analysis showed no significant chemical differences between them (Supporting Information, Section 6.1); however, GPC analysis revealed the recycled polymer contained higher molecular weight species (Table S5, Figure S26). We considered two explanations for this phenomenon. One possibility is that Zn^{2+} cations from solubilized ZnO act as ionic cross-linkers; therefore, some polymer chains contain additional cross-links. The other possibility is that some irreversible covalent bonds might have formed, such as thioether bonds from the desulfurization of disulfides. Nevertheless, the recycled mercapto-PMMA could still be used to synthesize a new gel via mechano-gelation, albeit half of the total polymer was replaced with virgin mercapto-PMMA to account for the lesser solubility of the recycled polymer (Figure 2). This new gel showed similar mechanical properties as the original one (Figure S29) and could also be dissolved with a TCEP solution. In addition, we conducted analogous experiments with the mercapto-PMA and mercapto-PS gels (Figure S25). The dissolution method with TCEP resulted in the parent polymers as characterized by GPC (Table S5, Figures S27 and 28). Unlike the case of mercapto-PMMA, the dissolution process of mercapto-PMA and mercapto-PS gels yielded polymers of nearly the same molecular weight as the virgin ones. Mercapto-PMA and mercapto-PS were recovered with yields of 83 and 90%, respectively, and reused to form new gels via mechano-cross-linking. Overall, these experiments showed the feasibility of reversing the mechano-gelation process and recycling the polymers.

Finally, we studied the mechanical and thermal properties of representative mechano-polymer composites obtained after drying the gel samples **a**, **f**, and **h**. In the case of the mercapto-PMMA composite (sample **a**), modulated DSC analysis showed a single broad T_g centered at 102 °C, as opposed to the sharp T_g of virgin mercapto-PMMA at 120 °C (Figure S35). As shown by the DMA temperature ramp experiment, the composite exhibited glassy behavior at room temperature, with an apparent storage modulus of 58 MPa and a broad T_g peaking at 128 °C (Figure 3). The modulus decreased to 0.8 MPa at 200 °C, but the sample did not melt. These results indicated that the composite was randomly cross-linked. Furthermore, a frequency sweep at 175 °C confirmed that it remained cross-linked at high temperature (Figure S38). In the case of the mercapto-PMA composite (sample **f**), modulated DSC showed one T_g nearly above room temperature (38 °C) and a broad T_g centered at 101 °C (Figure S36). The same lower temperature T_g was observed in virgin mercapto-PMA, albeit that it was a much sharper transition. The DMA temperature ramp experiment showed likewise both transitions. The composite exhibited glassy behavior at room temperature, with an apparent storage modulus of 29 MPa. However, it rapidly softened upon heating and plateaued at approximately 3 MPa between 50 and 100 °C. It then underwent a second, broad transition centered at 140 °C, and the modulus drastically dropped to 0.1 MPa (Figure 3). Although a frequency sweep at 175 °C confirmed the composite remained cross-linked, it had lost its original consistency (Figure S38). These results suggest that some regions of the composite are not cross-linked, thus behaving similarly to the parent polymer. Finally, in the case of the mercapto-PS composite (sample **h**), modulated DSC showed a single T_g centered at 114 °C (Figure S37), while DMA showed it at 130 °C (Figure 3). The sample retained its glassy state up

https://doi.org/10.1021/acsmacrolett.1c00337
ACS Macro Lett. 2021, 10, 799−804

to 100 °C with an apparent storage modulus of 10 MPa. It would then undergo a transition, with the modulus decreasing and plateauing at 0.9 MPa at 200 °C. As in the previous cases, a frequency sweep at 175 °C confirmed the composite remained cross-linked at high temperature (Figure S38).

In conclusion, we have demonstrated a new methodology that relies on mechanical force coupled with piezoelectrochemistry to fabricate reversible organogels via disulfide bond formation. Gels within a range of elastic moduli were obtained from three different polymers with thiol side groups. Mechanical activation and subsequent gelation of the mercapto-polymers was achieved with both high (40 kHz ultrasound) and low (2 kHz shaking) frequency sources of vibration. Chemical analysis conducted on a small molecule thiol confirmed that KI and ZnO could generate oxidation promoters under mechanical agitation, which could then oxidize the thiols to disulfides. A reversibility experiment showed that the gelation could be dissolved by treatment with a reducing agent and that the mercapto-polymers could be recycled for another round of mechano-cross-linking. Finally, we examined the diverse mechanical and thermal properties of the mercapto-polymer composites. We envision that this investigation will serve as the basis to generate adaptive materials with self-remodeling and self-healing properties by harnessing mechanical energy via piezoelectrochemistry.

■ ASSOCIATED CONTENT

Supporting Information

The Supporting Information is available free of charge at https://pubs.acs.org/doi/10.1021/acsmacrolett.1c00337.

Monomer and polymer synthesis schemes and chemical, mechanical and thermal characterization data of polymers, gels and composites (PDF)

■ AUTHOR INFORMATION

Corresponding Author

Aaron P. Esser-Kahn − *Pritzker School of Molecular Engineering, University of Chicago, Chicago, Illinois 60637, United States;* orcid.org/0000-0003-1273-0951; Email: aesserkahn@uchicago.edu

Authors

Jorge Ayarza − *Pritzker School of Molecular Engineering, University of Chicago, Chicago, Illinois 60637, United States;* orcid.org/0000-0002-1678-4503

Zhao Wang − *Pritzker School of Molecular Engineering, University of Chicago, Chicago, Illinois 60637, United States;* orcid.org/0000-0003-3226-3908

Jun Wang − *Pritzker School of Molecular Engineering, University of Chicago, Chicago, Illinois 60637, United States*

Complete contact information is available at: https://pubs.acs.org/10.1021/acsmacrolett.1c00337

Notes

The authors declare no competing financial interest.

■ ACKNOWLEDGMENTS

This work is supported by the US Air Force Office of Scientific Research (AFOSR) through Grant COE 5-29168, the National Science Foundation (NSF) through Grant CHE-1710116, the US Army Research Office (ARO) through Grant W911NF-17-1-0598 (71524-CH), and the University of Chicago Materials Research Science and Engineering Center (MRSEC), which is funded by the NSF under Award Number DMR-2011854. Parts of this work were carried out at the Soft Matter Characterization Facility (SMCF) and MRSEC facilities of the University of Chicago. We thank Dr. Philip J. Griffin, technical manager of SMCF, for helpful discussions.

■ REFERENCES

(1) Staudinger, H.; Heuer, W. Highly Polymerized Compounds. XCIII. The Breaking Up of the Molecular Fibers of the Polystyrenes. *Ber. Dtsch. Chem. Ges. B* **1934**, *67*, 1159−1164.

(2) Melville, H. W.; Murray, A. J. R. The Ultrasonic Degradation of Polymers. *Trans. Faraday Soc.* **1950**, *46*, 996−1009.

(3) Culter, J. D.; Zakin, J. L.; Patterson, G. K. Mechanical Degradation of Dilute Solutions of High Polymers in Capillary Tube Flow. *J. Appl. Polym. Sci.* **1975**, *19*, 3235−3240.

(4) Horn, A. F.; Merrill, E. W. Midpoint Scission of Macromolecules in Dilute Solution in Turbulent Flow. *Nature* **1984**, *312*, 140−141.

(5) Suslick, K. S.; Price, G. J. Applications of Ultrasound to Materials Chemistry. *Annu. Rev. Mater. Sci.* **1999**, *29*, 295−326.

(6) Dultsev, F. N.; Ostanin, V. P.; Klenerman, D. Hearing Bond Breakage. Measurement of Bond Rupture Forces Using a Quartz Crystal Microbalance. *Langmuir* **2000**, *16*, 5036−5040.

(7) Sohma, J. Mechanochemistry of Polymers. *Prog. Polym. Sci.* **1989**, *14*, 451−596.

(8) Caruso, M. M.; Davis, D. A.; Shen, Q.; Odom, S. A.; Sottos, N. R.; White, S. R.; Moore, J. S. Mechanically-induced Chemical Changes in Polymeric Materials. *Chem. Rev.* **2009**, *109*, 5755−5798.

(9) Black, A. L.; Orlicki, J. A.; Craig, S. L. Mechanochemically triggered bond formation in solid-state polymers. *J. Mater. Chem.* **2011**, *21*, 8460−8465.

(10) Black, A. L.; Lenhardt, J. M.; Craig, S. L. From Molecular Mechanochemistry to Stress-Responsive Materials. *J. Mater. Chem.* **2011**, *21*, 1655−1663.

(11) Ramirez, A. L. B.; Kean, Z. S.; Orlicki, J. A.; Champhekar, M.; Elsakr, s. M.; Krause, W. E.; Craig, S. L. Mechanochemical strengthening of a synthetic polymer in response to typically destructive shear forces. *Nat. Chem.* **2013**, *5*, 757−761.

(12) Wang, J.; Piskun, I.; Craig, S. L. Mechanochemical Strengthening of a Multi-mechanophore Benzocyclobutene Polymer. *ACS Macro Lett.* **2015**, *4*, 834−837.

(13) Li, J.; Nagamani, C.; Moore, J. S. Polymer Mechanochemistry: From Destructive to Productive. *Acc. Chem. Res.* **2015**, *48*, 2181−2190.

(14) Zhang, H.; Gao, F.; Cao, X.; Li, Y.; Xu, Y.; Weng, W.; Boulatov, R. Mechanochromism and Mechanical-Force-Triggered Cross-Linking from a Single Reactive Moiety Incorporated into Polymer Chains. *Angew. Chem., Int. Ed.* **2016**, *55*, 3040−3044.

(15) Matsuda, T.; Kawakami, R.; Namba, R.; Nakajima, T.; Gong, J. P. Mechanoresponsive self-growing hydrogels inspired by muscle training. *Science* **2019**, *363*, 504−508.

(16) Orrego, S.; Chen, Z.; Krekora, U.; Hou, D.; Jeon, S.-Y.; Pittman, M.; Montoya, C.; Chen, Y.; Kang, S. H. Bioinspired Materials with Self-Adaptable Mechanical Properties. *Adv. Mater.* **2020**, *32*, 1906970.

(17) Mohapatra, H.; Kleiman, M.; Esser-Kahn, A. P. Mechanically Controlled Radical Polymerization Initiated by Ultrasound. *Nat. Chem.* **2017**, *9*, 135−139.

(18) Wang, Z.; Pan, X.; Yan, J.; Dadashi-Silab, S.; Xie, G.; Zhang, J.; Wang, Z.; Xia, H.; Matyjaszewski, K. Temporal Control in Mechanically Controlled Atom Transfer Radical Polymerization Using Low ppm of Cu Catalyst. *ACS Macro Lett.* **2017**, *6*, 546−549.

(19) Wang, Z.; Pan, X.; Li, L.; Fantin, M.; Yan, J.; Wang, Z.; Wang, Z.; Xia, H.; Matyjaszewski, K. Enhancing Mechanically Induced ATRP by Promoting Interfacial Electron Transfer from Piezoelectric Nanoparticles to Cu Catalysts. *Macromolecules* **2017**, *50*, 7940−7948.

(20) Mohapatra, H.; Ayarza, J.; Sanders, E. C.; Scheuermann, A. M.; Griffin, P. J.; Esser-Kahn, A. P. Ultrasound Promoted Step-Growth

Polymerization and Polymer Crosslinking Via Copper Catalyzed Azide−Alkyne "Click" Reaction. *Angew. Chem., Int. Ed.* **2018**, *57*, 11208−11212.
(21) Wang, Z.; Ayarza, J.; Esser-Kahn, A. P. Mechanically Initiated Bulk-Scale Free-Radical Polymerization. *Angew. Chem., Int. Ed.* **2019**, *58*, 12023−12026.
(22) Ayarza, J.; Wang, Z.; Wang, J.; Huang, C.; Esser-Kahn, A. P. 100th Anniversary of Macromolecular Science Viewpoint: Piezoelectrically Mediated Mechanochemical Reactions for Adaptive Materials. *ACS Macro Lett.* **2020**, *9*, 1237−1248.
(23) Wang, Z.; Wang, J.; Ayarza, J.; Steeves, T.; Hu, Z.; Manna, S.; Esser-Kahn, A. P. Bio-inspired mechanically adaptive materials through vibration-induced crosslinking. *Nat. Mater.* **2021**, *20*, 869−874.
(24) Wojtecki, R. J.; Meador, M. A.; Rowan, S. J. Using the Dynamic Bond to Access Macroscopically Responsive Structurally Dynamic Polymers. *Nat. Mater.* **2011**, *10*, 14−27.
(25) Roy, D.; Cambre, J. N.; Sumerlin, B. S. Future Perspectives and Recent Advances in Stimuli-Responsive Materials. *Prog. Polym. Sci.* **2010**, *35*, 278−301.
(26) Hager, M. D.; van der Zwaag, S.; Schubert, U. S. *Self-Healing Materials*; Advances in Polymer Science 273; Springer: 2016.
(27) Yoon, J. A.; Kamada, J.; Koynov, K.; Mohin, J.; Nicolaÿ, R.; Zhang, Y.; Balazs, A. C.; Kowalewski, T.; Matyjaszewski, K. Self-Healing Polymer Films Based on Thiol-Disulfide Exchange Reactions and Self-Healing Kinetics Measured Using Atomic Force Microscopy. *Macromolecules* **2012**, *45*, 142−149.
(28) Fritze, U. F.; Craig, S. L.; von Delius, M. Disulfide-Centered Poly(Methyl Acrylates): Four Different Stimuli to Cleave a Polymer. *J. Polym. Sci., Part A: Polym. Chem.* **2018**, *56*, 1404−1411.
(29) Fritze, U. F.; von Delius, M. Dynamic disulfide metathesis induced by ultrasound. *Chem. Commun.* **2016**, *52*, 6363−6366.
(30) García Ruano, J. L.; Parra, A.; Alemán, J. Efficient synthesis of disulfides by air oxidation of thiols under sonication. *Green Chem.* **2008**, *10*, 706−711.
(31) Mirzahosseini, A.; Noszál, B. Species-Specific Standard Redox Potential of Thiol-Disulfide Systems: A Key Parameter to Develop Agents against Oxidative Stress. *Sci. Rep.* **2016**, *6*, 37596.
(32) Kröger, A. P. P.; Boonen, R. J. A. E.; Paulusse, J. M. J. Well-defined single-chain polymer nanoparticles via thiol-Michael Addition. *Polymer* **2017**, *120*, 119−128.
(33) Kirihara, A.; Asai, Y.; Ogawa, S.; Noguchi, T.; Hatano, A.; Hirai, Y. A Mild and Environmentally Benign Oxidation of Thiols to Disulfides. *Synthesis* **2007**, *2007*, 3286−3289.
(34) Sandmann, A.; Kompch, A.; Mackert, V.; Liebscher, C. H.; Winterer, M. Interaction of L-Cysteine with ZnO: Structure, Surface Chemistry, and Optical Properties. *Langmuir* **2015**, *31*, 5701−5711.
(35) Sadik, P. W.; Pearton, S. J.; Norton, D. P.; Lambers, E.; Ren, F. Functionalizing Zn- and O-terminated ZnO with thiols. *J. Appl. Phys.* **2007**, *101*, 104514.
(36) Guglieri, C.; Aquilanti, G.; Díaz-Moreno, S.; Chaboy, J. Determination of the S−ZnO structural interaction in thiol-capped ZnO nanoparticles: a sulfur K-edge XAS study. *Nanotechnology* **2017**, *28*, 055704.
(37) Dvorak, J.; Jirsak, T.; Rodriguez, J. A. Fundamental studies of desulfurization process: reaction of methanethiol on ZnO and Cs/ZnO. *Surf. Sci.* **2001**, *479*, 155−168.

https://doi.org/10.1021/acsmacrolett.1c00337
ACS Macro Lett. 2021, 10, 799−804